These two qualitatively different kinds of bending potentials seem to indicate the possibility of two kinds of moieties that might be identifiable in oxycumulenes in general. The first is a ketene-type moiety (=C=C=O), which favors a linear structure. The second is an allene-type structure (=C=C=C=), which also favors a linear configuration. At the juncture of these moieties, however, low bending force constants may be found. This would lead to a general view of oxycumulenes as

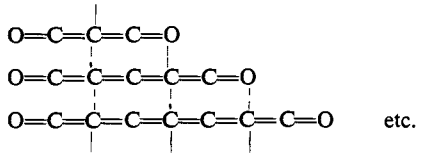

where facile bending would be expected at the carbon atoms that join the ketene and allene moieties. However, considerable further investigation may be needed to test the generality of this notion.

Acknowledgments. The authors express their gratitude to G. M. Maggiora and L. L. Shipman for many helpful discussions and contributions to this work. Support to L. W. from the exchange program with the University of Poznan, Poland, is gratefully acknowledged. Also, the authors thank the University of Kansas for partial support of the computing time required for this work, and R. E. C. expresses his appreciation to W. N. Lipscomb for his generous hospitality and stimulating conversations concerning this work.

Electrostatic Force Theory for a Molecule and Interacting Molecules. III. Overlap Effect on the Atomic Dipole and Exchange Forces, Orbital Following and Preceding, and the Shapes of X_mABY_n Molecules

Hiroshi Nakatsuji

Contribution from the Department of Hydrocarbon Chemistry, Faculty of Engineering, Kyoto University, Kyoto, Japan.
Received September 19, 1972

Abstract: This paper treats an extension of the electrostatic force (ESF) theory proposed previously.[1] First, the effect of orbital overlap (named *overlap effect*) on the atomic dipole (AD) and exchange (EC) forces is examined. The effect is proved to have wide applicabilities for both molecular structure and chemical reaction. Especially the π-overlap effect may be considered as the "conjugation effect" in comparison with the inductive substituent effects on the AD and EC forces summarized previously. Moreover, the overlap effect on the EC force manifests itself in many important aspects of chemical reaction and molecular interaction (*e.g.*, conservation of molecular orbital symmetry, non-least-motion reaction path, exchange repulsion, etc.). Another manifestation of the overlap effect is the orbital following and preceding in the problem of internal rotation barrier. Generally, the *orbital following*, which means the incomplete following of (local) electron distribution to a movement of nuclei, causes forces that *restrain* the movement of nuclei. On the other hand, the *orbital preceding*, which means the preceding of (local) electron distribution to a movement of nuclei, causes forces that *promote* the movement of nuclei. These orbital following and preceding are proved to be a dominant origin of the rotational barrier in many important cases except for the internal rotation about the single bond. General features in the internal rotation about the single bond are also studied, and three factors are pointed out as important. Based on the ESF theory reinforced by the above considerations, the shapes of X_mABY_n molecules are discussed. The results are generally satisfactory.

In the previous two papers of this series,[1] the electrostatic force (ESF) theory in which chemical phenomena are studied through force concept (not through energetics) has been developed and applied mainly to the shapes of the ground and excited states of a wide variety of AX_n molecules. The basis of the theory is the Hellmann–Feynman theorem[2,3] expressed in atomic units by

$$\mathbf{F}_A = Z_A\left\{\int \rho(\mathbf{r}_1)\mathbf{r}_{A_1}/r_{A_1}^3\,d\mathbf{r}_1 - \sum_{B(\neq A)} Z_B\mathbf{R}_{AB}/R_{AB}^3\right\} \quad (1)$$

with the same notations as in paper I. Taking advantage of the physical simplicity and visuality of eq 1, we derived three pictorial concepts called atomic dipole (AD) force, exchange (EC) force, and gross charge (GC) or extended gross charge (EGC) force. The balancing of these forces determines molecular shape. Some regularities in the influences on these forces induced by the change of the concerned atom A and substituent X were summarized. Especially, the shapes of usual molecules were shown to be in close relation with the electron density in the p_π AO of the central atom A in planar or linear structures, which is designated as $D(p_{\pi A})$ (see Figure 7 of paper I). These theoretical concepts were shown to be very useful in predicting the shapes of molecules in both the ground and

(1) H. Nakatsuji, *J. Amer. Chem. Soc.*, **95**, 345, 354 (1973), which are referred to in the text as papers I and II, respectively.
(2) H. Hellmann, "Einführung in die Quantenchemie," Deuticke, Vienna, 1937; R. P. Feynman, *Phys. Rev.*, **56**, 340 (1939).
(3) A. C. Hurley, "Molecular Orbitals in Chemistry, Physics and Biology," P.-O. Löwdin and B. Pullman, Ed., Academic Press, New York, N. Y., p 161; *Proc. Roy. Soc., Ser. A*, **226**, 170, 179 (1954).

Table I. Overlap Effect

Interaction	$D(p_{\pi A})$ AD force	EC force[a,b]	Corresponding phenomena: Molecular shape[c]	Chemical reaction
Bonding interaction[d]	$\frac{1}{1+S}$	$\frac{2}{1+S}I_{EC}$	Linear or planar	Driving force: Conservation of molecular orbital symmetry
Antibonding interaction[e]	$\frac{1}{1-S}$	$-\frac{2}{1-S}I_{EC}$	Bent or pyramidal	Repulsive force: Conservation of molecular orbital symmetry
Interaction between fully occupied AO's	$\frac{2}{1-S^2}$	$-\frac{4S}{1-S^2}I_{EC}$	Bent or pyramidal	Repulsive force: (i) Non-least-motion reaction path; (ii) Exchange repulsion

[a] $I_{EC} = \langle \chi_{rA} | (r_A/r_A^3)_0 | \chi_{sB} \rangle$. The prefactor of I_{EC} is the bond order between χ_{rA} and χ_{sB}. [b] Plus and minus signs correspond to the attractive and repulsive forces between A and B. [c] On the role of the σ-overlap effect see the text. [d] The values correspond to the electronic configuration $(\varphi_b)^2(\varphi_a)^0$. [e] The values correspond to the electronic configuration $(\varphi_b)^0(\varphi_a)^2$.

excited states and in understanding the natures of chemical reactions and the structures of products.

In the present paper, we intend an extension of the ESF theory. First, the effect of orbital overlap on the AD and EC forces is examined. The effect (named *overlap effect*) has a general importance for both problems of molecular structure and chemical reaction. Another manifestation of the overlap effect is the orbital following and preceding in the problems of internal rotation. They are shown to be the dominant origin of rotational barriers in many important cases. The internal rotation about a single bond is discussed separately. The ESF theory reinforced by these considerations is then applied to the shapes of X_mABY_n molecules.

The shapes of X_mABY_n molecules have also been treated by other general theories of molecular structure. The representatives are the method of orbital correlation diagram, due originally to Walsh[4] and recently reexamined by Gimarc,[5] and the second-order Jahn–Teller (SOJT) theory due to Pearson.[6] In any theories, these molecules have a critical importance in the extension of the applicability of the theory from AX_n molecules to general $AX_k(BY_l)_mCZ_n$ molecules.

Overlap Effect on the AD and EC Forces

The effect of orbital overlap on binding energy, electron-density distribution, etc., has been widely investigated from early days of quantum chemistry. Since the effect has a general importance for both problems of molecular structure and chemical reaction, it is reexamined here from the present theoretical standpoint.[7] The effect will be called hereafter the *overlap effect.*

If two AO's χ_{rA} and χ_{sB} approach each other until they have overlap interactions, the wave function of the system may be written approximately with the following bonding and antibonding MO's

$$\varphi_b = (\chi_{rA} + \chi_{sB})/(2 + 2S)^{1/2}$$
$$\varphi_a = (\chi_{rA} - \chi_{sB})/(2 - 2S)^{1/2} \qquad (2)$$

where the atoms A and B are assumed to be homopolar[8] and S is the overlap integral between the AO's χ_{rA} and χ_{sB}. The physical picture of eq 2 is that, in the bonding orbital, electron(s) in these AO's flow(s) into the A–B bond region, but in the antibonding orbital, the reverse occurs due to the existence of a node. In Table I, the effects of orbital overlap on the AD and EC forces are summarized. The second column shows the contributions to $D(p_{\pi A})$ from doubly occupied π-bonding and π-antibonding MO's and the sum of them (the interaction between fully occupied AO's). Since the magnitude of $D(p_{\pi A})$ is approximately parallel to the AD force acting on atom A for usual molecules,[1] it may well be considered as the effect on the AD force. The third column shows the effect on the EC force. Plus and minus signs correspond to attractive and repulsive forces, respectively. Summaries of the resultant effects and the corresponding phenomena are also given for molecular structure and chemical reaction.

First, the overlap effect on molecular structure is discussed. It is convenient to divide it to π- and σ-overlap effects. By the occurrence of π-bonding interaction between singly occupied AO's, $D(p_{\pi A})$ decreases from unity to $1/(1+S)$, and then the AD force diminishes, but the EC force increases. These effects cooperatively function to make the shape near atom A linear or planar. The effect of the π-antibonding interaction is the reverse of that of the π-bonding interaction and thus advantageous for bent or pyramidal structures. When both AO's χ_{rA} and χ_{sB} are doubly occupied, the effect of π antibonding surpasses the effect of π bonding. For more than two π-AO systems, the generalization of Table I is very easy.[9] Note that for nonbonding interaction, the overlap effects on both the AD and EC forces are approximately zero. Coulson generalized the fact that completely filled MO shells lead to negative bond orders to many AO cases.[10] These π-overlap effects may be considered as the "conjugation effects" in comparison with the inductive substituent effects on the AD and EC forces summarized in paper I.

The σ-overlap effect is very similarly discussed. By the increase in the σ-bonding interaction, the electron cloud in s_A AO flows into the bond region, and at the same time the s_A–s_B bonding MO is stabilized and the

(4) A. D. Walsh, *J. Chem. Soc.*, 2260, 2266, 2288, 2296, 2301, 2306, 2321, 2325 (1953).
(5) B. M. Gimarc, *J. Amer. Chem. Soc.*, **92**, 266 (1970); **93**, 593, 815 (1971).
(6) R. G. Pearson, *J. Chem. Phys.*, **52**, 2167 (1970); *J. Amer. Chem. Soc.*, **91**, 1252, 4947 (1969); *Chem. Phys. Lett.*, **10**, 31 (1971).
(7) Some aspects of the overlap effect have been mentioned already in paper II in the section of HAX molecules and part of the overlap effect on the EC force was given as the effect of bond multiplicity.
(8) For heteropolar cases, the overlap effect becomes generally smaller. The inductive substituent effects on the AD and EC forces summarized previously[1] are also helpful in this case.
(9) See, for example, A. Streitwieser, Jr., "Molecular Orbital Theory for Organic Chemists," Wiley, New York, N. Y., 1961.
(10) C. A. Coulson, *Mol. Phys.*, **15**, 317 (1968).

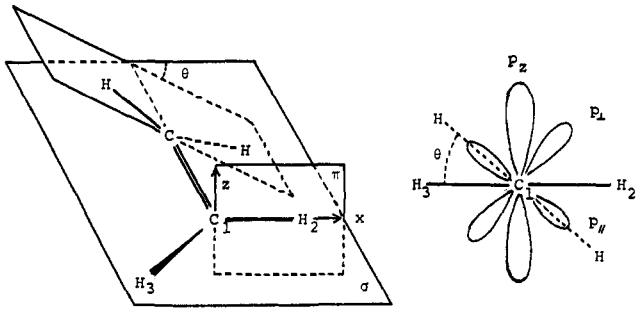

Figure 1. The ethylene molecule twisted by the angle θ. The right-hand side is the Newman-type diagram. Front-side and back-side CH_2 fragments are shown by solid and dashed lines, respectively. p_z AO on the front-side CH_2 fragment is decomposed into $p_\perp$ and $p_{||}$ AO's. (The notations $\perp$ and $||$ are used with respect to the back-side CH_2 plane.)

s_A–s_B antibonding MO is destabilized. These effects cause the extent of s–p hybridization at atom A to decrease[1] and then the AD force to decrease. But the EC force increases. Thus, the increase in the σ-bonding overlap interaction operates to make the shape linear or planar. The effect of σ-antibonding is reverse to that of the σ-bonding interaction. Thus, the σ-overlap effect is parallel with the π-overlap effect for molecular shape.

If the extent of change in σ overlap from the reference molecules[11] is very large, the critical value of $D(p_{\pi A})$ in the linear-bent problem shown in Figure 7 of paper I will suffer some change. For example, if the σ-bonding interaction in the A–X bond is much larger than that in the A–H bond, the shape near atom A will be linear or planar even if $D(p_{\pi A})$ is to some extent larger than unity.

For chemical reaction, the overlap effect on the EC force is very important.[1] The bonding interaction between χ_{rA} and χ_{sB} results in an attractive force, but the antibonding interaction and the interaction between fully occupied AO's cause a repulsive force. These effects are important in the study of reaction path. For example, the fact that the signs of the AO's are the same for the bonding interaction but different for the antibonding interaction leads to the well-known rule of orbital symmetry conservation.[12,13] Actually, a similar formulation on the symmetry rule derived by Salem[14] and Pearson[13] is possible from the Hellmann–Feynman theorem.[15] The "overlap stabilization" proposed by Fukui[16,17] is an energetic expression of the overlap effect on the EC force. The repulsive EC force between two fully occupied AO's expresses the exchange repulsion energy in the field of intermolecular force[18] and corresponds to the "exclusion shell" proposed by Salem.[19] This is also one of the most important factors in discussing the non-least-motion reaction path studied by Hoffmann, *et al.*[20] These points will be examined more fully in the succeeding papers.[21]

Orbital Following and Preceding and Rotational Force

In going from AX_n molecules to X_mABY_n molecules, the problem concerning the rotational freedom about the A–B (single, double, or triple) bond arises. The main purpose of this section is to point out one of the important aspects of electron-density distribution, namely orbital following and orbital preceding, which are in many important cases the dominant origins of internal rotation barriers. These pictures obtained from the ESF theory are quite different from those obtained from usual energetic considerations. The rotational problem about the single bond[22] will be discussed separately in the following section.

Let us start the discussion by using a typical example of the ethylene molecule. Figure 1 shows the ethylene molecule twisted by an angle θ. The energetic account of the planarity is that the stabilization due to the π-bonding interaction between two $p_{\pi C}$ AO's is maximum in this structure.[23] On the other hand, the account from the ESF theory is as follows. The interest is focused on the C_1–H_2 bond-electron distribution. When p_z AO of the front-side CH_2 fragment is decomposed into $p_\perp$ and $p_{||}$ AO's as shown in Figure 1, the electron cloud in $p_\perp$ AO flows into the C–C bond region owing to the bonding overlap interaction with the p_π AO on the back-side CH_2,[24] while that in $p_{||}$ AO suffers little change.[24] As a result, the bond-electron distribution along the C_1–H_2 bond is deformed as illustrated by

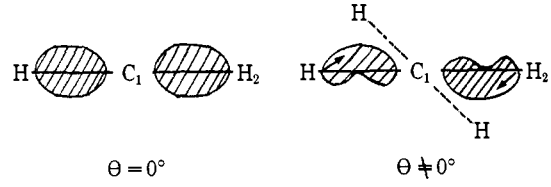

The deformed bond-electron distribution shown above causes the EC force which operates as a restoring rotational force to the planar structure as shown by the arrows.

Namely, in ethylene the C–H bond-electron distribution follows incompletely to the twisting motion of C–H nuclei. This is an example of *orbital following* and causes a main restoring force to planar structure. The reverse phenomenon, that the C–H bond-electron distribution precedes to the twisting motion of C–H nuclei, is an example of *orbital preceding*, which causes

(11) The critical values of $D(p_{\pi A})$ shown in Figure 7 of paper I were determined with reference to the experimental shapes of $CH_2(^3B_1)$ and CH_3. See also Table I of paper I.

(12) (a) R. B. Woodward and R. Hoffmann, *Angew. Chem.*, **81**, 797 (1969); "The Conservation of Orbital Symmetry," Academic Press, New York, N. Y., 1969, and their preceding papers cited therein; (b) K. Fukui, "Theory of Orientation and Stereoselection," Springer Verlag, Heidelberg, 1970.

(13) R. G. Pearson, *Theor. Chim. Acta*, **16**, 107 (1970); *Accounts Chem. Res.*, **4**, 152 (1971).

(14) L. Salem, *Chem. Phys. Lett.*, **3**, 99 (1969); see also R. F. W. Bader, *Mol. Phys.*, **3**, 137 (1960); *Can. J. Chem.*, **40**, 1164 (1962).

(15) H. Nakatsuji, unpublished result.

(16) K. Fukui, *Bull. Chem. Soc. Jap.*, **39**, 498 (1966).

(17) K. Fukui and H. Fujimoto, *ibid.*, **41**, 1989 (1968); **42**, 3399 (1969); H. Fujimoto, S. Yamabe, and K. Fukui, *ibid.*, **44**, 2936 (1971).

(18) See, for example, J. O. Hirschfelder, Ed., *Advan. Chem. Phys.*, **12**, 329 (1967).

(19) L. Salem, *J. Amer. Chem. Soc.*, **90**, 543 (1968).

(20) R. Hoffmann, R. Gleiter, and F. B. Mallory, *ibid.*, **92**, 1460 (1970).

(21) (a) H. Nakatsuji, T. Kuwata, and A. Yoshida, to be submitted for publication; (b) H. Nakatsuji, to be submitted for publication.

(22) (a) E. B. Wilson, *Advan. Chem. Phys.*, **2**, 367 (1959); (b) J. P. Lowe, *Progr. Phys. Org. Chem.*, **6**, 1 (1968); (c) L. C. Allen, *Annu. Rev. Phys. Chem.*, **20**, 315 (1969).

(23) R. S. Mulliken, *Phys. Rev.*, **41**, 751 (1932); **43**, 279 (1933); *Rev. Mod. Phys.*, **14**, 265 (1942).

(24) Flotation of the electron cloud into the C-C bond region can be measured by bond order. For example, the bond order between $p_\perp$ AO and the p_π AO of the back-side CH_2 is approximately $2/(1 + S) \simeq 1.6$, but the bond order between $p_{||}$ AO and the C-H bond orbital of the back-side CH_2 is approximately $(1 - 3S)/(1 - S^2) \simeq 0.1$ (refer to Table I).

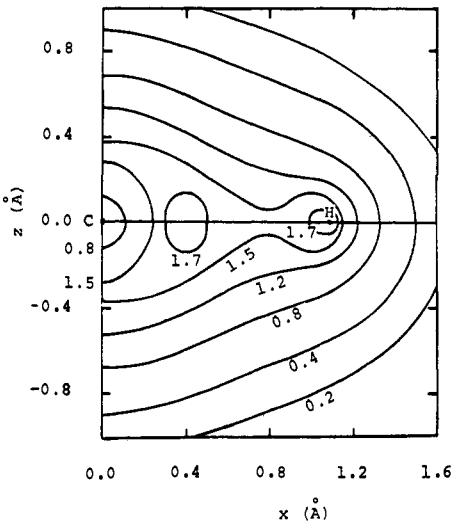

Figure 2. The density map along the C_1–H_2 bond on the π plane for the configuration $(\pi)^2(\pi^*)^0$ at $\theta = 0°$.

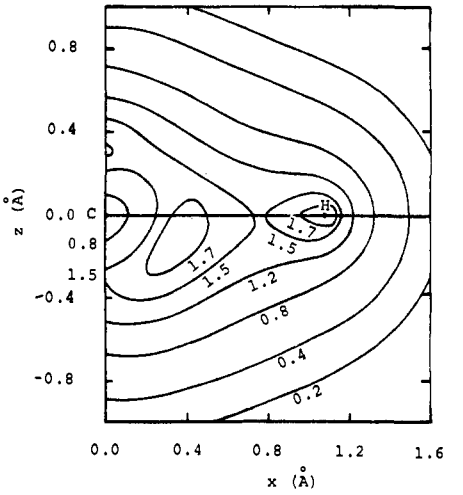

Figure 3. The density map along the C_1–H_2 bond on the π plane for the configuration $(\pi)^2(\pi^*)^0$ at $\theta = 45°$.

a main rotational force to make, *e.g.*, π–π^* excited states of ethylene[25] and BH_2BH_2[26] and its derivatives (*e.g.*, B_2F_4,[27] B_2Cl_4[28]) to take the bisected structure.

In order to confirm the above statements, we present in Figures 2–7 the electron-density maps along the C_1–H_2 bond on the π plane (see Figure 1) calculated from the extended Hückel MO's of ethylene, and in Table II the rotational force acting on H_2.[29] Figure 2 is

Table II. Analyses of the Rotational Force, $F_z(H_2)$ (au), at $\theta = 45°$ for Various Electronic Configurations Arising from Ethylenic MO's[a]

Force	Electronic configuration $(\pi)^2(\pi^*)^0$	$(\pi)^1(\pi^*)^1$	$(\pi)^0(\pi^*)^0$	$(\pi)^2(\pi^*)^2$
Total	−0.0262	0.0178	0.0300	0.0056
	(i) First Analysis (Eq 3)			
Electronic part	−0.0303	0.0137	0.0259	0.0015
Nuclear part	0.0041	0.0041	0.0041	0.0041
	(ii) Second Analysis (Eq 4)			
EC(C_1–H_2) force	−0.0286	0.0144	0.0202	0.0086
EC(other) force	0.0012	0.0005	0.0024	−0.0014
EGC force	0.0012	0.0028	0.0073	−0.0017

[a] See Figure 1.

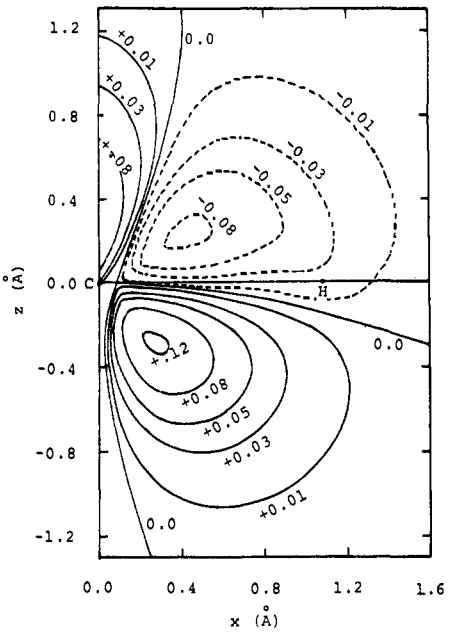

Figure 4. The change in the density distribution along the C_1–H_2 bond on the π plane induced by the twisting motion at $\theta = 45°$ for the configuration $(\pi)^2(\pi^*)^0$.

the density map at $\theta = 0°$. The density is symmetrical about the x axis. But, when $\theta = 45°$ (Figure 3), the orbital following occurs certainly. The density flows from the $+z$ region to the $-z$ region. This is more easily seen in Figure 4 which shows the *change* in the electron-density distribution induced by the twisting motion at $\theta = 45°$. On the other hand, orbital preceding is seen in Figures 5 and 6 for $(\pi)^1(\pi^*)^1$ and $(\pi)^0(\pi^*)^0$ configurations which correspond to the π–π^* excited states of ethylene and to BH_2BH_2 and its derivatives, respectively. The conclusion that orbital following and preceding are the *dominant* origin of the rotational forces in these molecules is ascertained from Table II, where the analysis of force is made in two alternative ways. The first is due to the equation

$$F_z(H_2) = \text{(electronic part)} + \text{(nuclear part)} \quad (3)$$

where the electronic and nuclear parts correspond respectively to the first and second terms of eq 1. The second is due to the analysis

$$F_z(H_2) = \text{EC}(C_1\text{–}H_2)\text{ force} + \text{EC(other) force} + \text{EGC force} \quad (4)$$

where the AD force on the proton is zero in the extended Hückel approximation. The EC(other) force means the EC force due to the overlap density between H_2 and all the other (nonbonded) nuclei except C_1. For $(\pi)^2(\pi^*)^0$, $(\pi)^1(\pi^*)^1$, and $(\pi)^0(\pi^*)^0$ configurations, the first analysis shows that the electronic part is the domi-

(25) R. G. Wilkinson and R. S. Mulliken, *J. Chem. Phys.*, **23**, 1895 (1955); R. McDiarmid and E. Charney, *ibid.*, **47**, 1517 (1967).
(26) A. A. Frost, quoted by R. G. Pearson, *ibid.*, **52**, 2167 (1970).
(27) J. N. Gayles and J. Self, *ibid.*, **40**, 3530 (1964).
(28) D. E. Mann and L. Fano, *ibid.*, **26**, 1665 (1957); K. Hedberg and R. R. Ryan, *ibid.*, **41**, 2214 (1964).
(29) All the integrals necessary for the force calculations shown in eq 5 of paper I were calculated exactly by using Slater valence AO's ($\zeta_C = 1.625$, $\zeta_H = 1.0$).

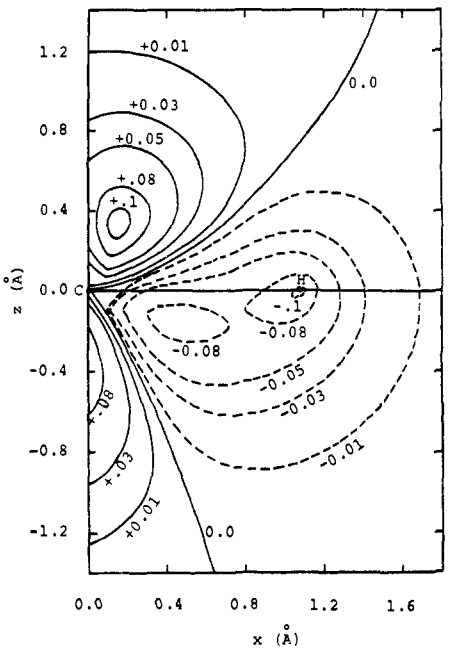

Figure 5. The change in the density distribution along the C_1–H_2 bond on the π plane induced by the twisting motion at $\theta = 45°$ for the configuration $(\pi)^1(\pi^*)^1$.

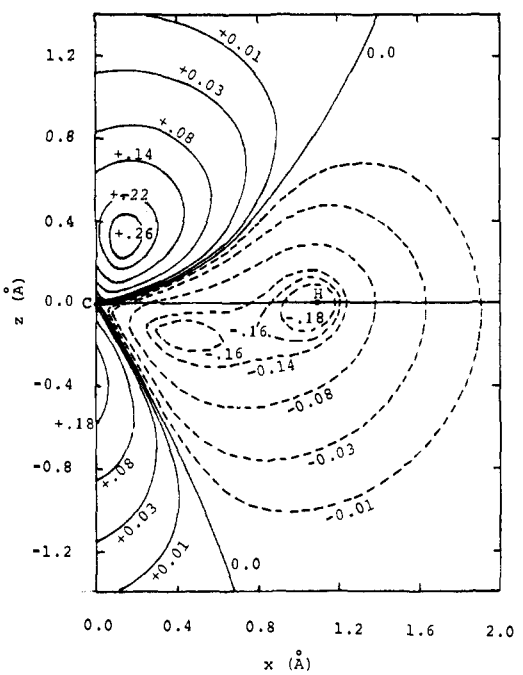

Figure 6. The change in the density distribution along the C_1–H_2 bond on the π plane induced by the twisting motion at $\theta = 45°$ for the configuration $(\pi)^0(\pi^*)^0$.

nant origin of the rotational force. Although the electronic part is the sum of various contributions, the second analysis shows clearly that the EC(C_1–H_2) force arising from the deformation of the C_1–H_2 bond-electron distribution illustrated in the above figure makes the predominant contribution. Although the extended Hückel wave function has many defects for the basis of force calculations,[21a] the general features of Figures 2–7 and Table II should not be altered by the more accurate calculations.

For $(\pi)^2(\pi^*)^2$ configurations, which are given for

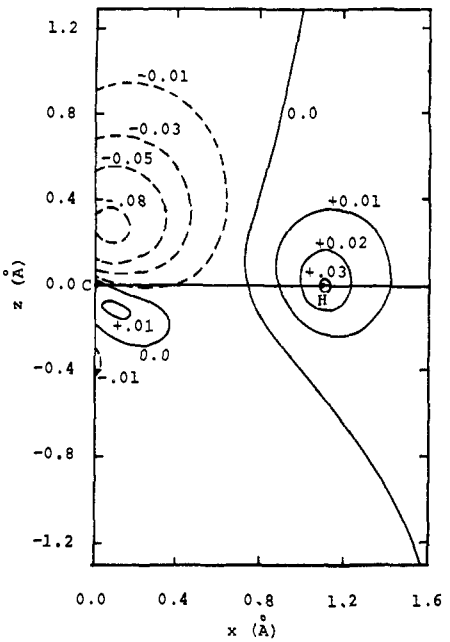

Figure 7. The change in the density distribution along the C_1–H_2 bond on the π plane induced by the twisting motion at $\theta = 45°$ for the configuration $(\pi)^2(\pi^*)^2$.

comparison with NH_2NH_2, the electronic part is smaller than the nuclear part. Actually, the change in the bond-electron distribution is relatively small as shown in Figure 7 (small orbital preceding). However, the resulting force is very important in the second analysis shown in Table II and cannot be neglected for sensitive problems like rotation about the single bond.

As may be clear from the above discussions, the orbital following and preceding in the rotational problem arise from the difference in the interactions (difference in the overlap effects) of the $p_\perp$ and $p_\parallel$ AO's with the electron cloud of the rotor of another side. Then, if the overlap density including $p_\perp$ AO is larger than that including $p_\parallel$ AO, the orbital following will occur. For the reverse case, the orbital preceding will occur. In these, the C–H bond orbital may be treated approximately as a fully occupied AO. For the rotation about a single bond, the interactions including $p_\perp$ and $p_\parallel$ AO's become similar in that both belong to the category of interactions between fully occupied AO's (see Table I). Then, the extent of the orbital following and preceding will become very small, and other small interactions should also be considered.

Hitherto, the possibility of the orbital following has sometimes been pointed out,[30] especially in the field of molecular vibration. Schrader and Karplus used this concept in order to account for the esr hfs constant and its temperature dependence of methyl and deuteriomethyl radicals.[31] More recently, Chang, Davidson, and Vincow showed the orbital following in methyl

(30) (a) J. W. Linnett and P. J. Wheatley, *Trans. Faraday Soc.*, **45**, 33, 39 (1949); (b) T. Itoh, K. Ohno, and M. Kotani, *J. Phys. Soc. Jap.*, **8**, 41 (1953); (c) N. V. Cohen and C. A. Coulson, *Trans. Faraday Soc.*, **52**, 1163 (1956); (d) D. C. McKean and P. N. Schatz, *J. Chem. Phys.*, **24**, 316 (1956); (e) C. A. Coulson and M. J. Stephens, *Trans. Faraday Soc.*, **53**, 272 (1957); (f) W. D. Jones and W. T. Simpson, *J. Chem. Phys.*, **32**, 1747 (1960); (g) P. C. H. Jordan and H. C. Longuet-Higgins, *Mol. Phys.*, **5**, 121 (1962).

(31) D. M. Schrader and M. Karplus, *J. Chem. Phys.*, **40**, 1593 (1964); D. M. Schrader, *ibid.*, 46, 3895 (1967); see also R. W. Fessenden, *J. Phys. Chem.*, 71, 74 (1967).

radical by *ab initio* calculations.[32] Since in the present ESF theory the knowledge on the manner of electron distribution has a predominant importance in comparison with other energetic theories (see eq 1), orbital following and preceding become so much the more important. Generally speaking, the orbital following, which means the incomplete following of the (local) electron cloud to a movement of nuclei, causes forces that *restrain* the movement of the nuclei. On the other hand, the orbital preceding causes forces that *promote* the movement of the nuclei. These phenomena are considered to have a general importance for problems including the movements of nuclei. Actually, the generality of the orbital following and preceding can be proved directly from the Hellmann–Feynman theorem (eq 1).[21b] A manifestation of the orbital preceding in a chemical reaction will be shown in the succeeding paper of this series.[21]

Rotation about the Single Bond

The origin of the barrier to internal rotation about the single bond has been a subject of extensive studies by means of various theoretical methods.[22,33-37] Among these, *ab initio* SCF-MO calculations seem most promising.[33,34,36c] From the analyses of these SCF-MO results, Allen[34] showed that the barrier mechanism can well be interpreted by using the energy components $V_{att} \equiv V_{ne}$ and $V_{rep} \equiv T + V_{nn} + V_{ee}$. His study may be considered as showing that pictorial understanding based on usual chemical knowledge is possible even of these sensitive problems.

In the present ESF theory, the following three factors are considered to be important for H_mABH_n molecules: (a) the orbital following and preceding, (b) the interaction of the concerned proton H_1 on one side with the B–H_2 bond on another side, and (c) the interaction of the concerned proton H_1 on one side with the lone-pair electrons on another side.

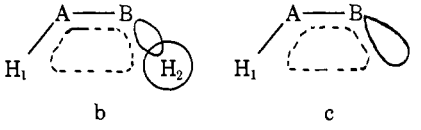

The above figures are the illustrations of interactions b and c. For the effect a, details are given above. The effect will be important for the A–B bond which has partial double bond character. The hyperconjugation effect[33i,38] will also be included in the effect a from the present standpoint. For the interaction b, the interaction between the H_1 proton and the electron cloud belonging to the B–H_2 bond and the H_2 atom (shown by the solid line) is attractive, but the force due to the electron cloud between H_1 and B–H_2 (shown by the dotted line) is attractive or repulsive. The H_1–H_2 bare-nuclear interaction is repulsive. With reference to the experimental and theoretical results given hitherto, *the total effect of the interaction b seems repulsive.* Allen[34] and Sovers, *et al.*,[35b] arrived at the conclusion that the repulsion between C–H bonds in ethane is closely similar to that between two helium atoms.[21a] For the interaction c, the interaction between the H_1 proton and the lone-pair electron cloud at B (shown by the solid line) is attractive, but the force due to the electron cloud intermediate between the H_1 and the lone-pair orbital (shown by the dotted line) is attractive or repulsive. However, for the actual molecules, the former attractive force is considered to be larger than the latter attractive or repulsive force, since the two-center coulombic integrals of the type $\langle \chi_{sB} | \mathbf{r}_H / r_H^3 | \chi_{sB} \rangle$ are usually larger than the net-exchange integrals of the type $\langle \chi_H | (\mathbf{r}_H / r_H^3)_0 | \chi_{sB} \rangle$ and the three-center integrals of the type $\langle \chi_{rA} | \mathbf{r}_H / r_H^3 | \chi_{sB} \rangle$,[39] and since the preintegral density matrix element is also larger for the former than for the latter two types. Then, *the total effect of the interaction c is thought to be attractive.* Note that the terms "repulsive dominant" and "attractive dominant" mechanisms used by Allen[34] are different from the classification of mechanisms given here from the ESF theory.

In Table III, the stable angles and barriers to internal rotation about the single bond are summarized for representative molecules. Although some of them belong to the types of molecules discussed in the following sections, it is convenient to summarize the discussions here. In order to determine the relative importance of the above factors for actual molecules, numerical calculations based on very accurate wave functions are indispensable.[35a] However, some of the qualitative features of the experimental conformations and barriers shown in Table III seem understandable from the above knowledge. In Figure 8 we picked out from Table III the representative molecules. For ethane, the factor b should be most important, and then the staggered form will be more favorable than the eclipsed form. For hydrogen peroxide, H_2O_2, both factors b and c should be considered. Especially since the oxygen atom has two lone-pairs—one lies in the HOO plane (σ lone pair) and the other is perpendicular to this plane (π lone pair),[40] the force acting on the H_1 proton in the trans region (θ = 90–180° from cis) seems to be determined by the delicate balance of the attractive interactions c with these two lone pairs. Although the attractive interaction with the π lone pair seems larger, since the π lone pair is nearer to H_1 than the σ lone pair, more reliable calculation is necessary

(32) S. Y. Chang, E. R. Davidson, and G. Vincow, *J. Chem. Phys.*, **52**, 5596 (1970); see also ref 30b.

(33) (a) R. M. Pitzer and W. N. Lipscomb, *J. Chem. Phys.*, **39**, 1955 (1963); (b) V. Kaldor and I. Shavitt, *ibid.*, **44**, 1823 (1966); (c) O. J. Sovers and M. Karplus, *ibid.*, **44**, 3033 (1966); (d) E. Clementi and D. R. Davis, *ibid.*, **45**, 2593 (1966); (e) A. Veillard, *Theor. Chim. Acta*, **5**, 413 (1966); (f) W. H. Fink and L. C. Allen, *J. Chem. Phys.*, **46**, 2261, 2276 (1967); (g) L. Pedersen and K. Morokuma, *ibid.*, **46**, 3941 (1967); (h) W. E. Palke and R. M. Pitzer, *ibid.*, **46**, 3948 (1967); (i) W. H. Fink, D. C. Pan, and L. C. Allen, *ibid.*, **47**, 895 (1967); (j) M. S. Schwartz, *ibid.*, **51**, 4182 (1969); (k) R. M. Stevens, *ibid.*, **52**, 1397 (1970).

(34) L. C. Allen, *Chem. Phys. Lett.*, **2**, 597 (1968).

(35) (a) J. Goodisman, *J. Chem. Phys.*, **44**, 2085 (1966); **45**, 4689 (1966); **47**, 334 (1967); (b) O. J. Sovers, C. W. Kern, R. M. Pitzer, and M. Karplus, *ibid.*, **49**, 2592 (1968).

(36) (a) R. E. Wyatt and R. G. Parr, *ibid.*, **41**, 3262 (1964); **43**, S217 (1965); (b) J. P. Lowe and R. G. Parr, *ibid.*, **44**, 3001 (1966); (c) W. H. Fink and L. C. Allen, *ibid.*, **46**, 3270 (1967).

(37) W. L. Jorgensen and L. C. Allen, *J. Amer. Chem. Soc.*, **93**, 567 (1971).

(38) G. Winnewisser, M. Winnewisser, and W. Gordy, *J. Chem. Phys.*, **49**, 3465 (1968).

(39) For HOOH, the values of the integrals $\langle p_{\bar{\pi}O'} | \sigma_H / r_H^3 | p_{\bar{\pi}O'} \rangle$, $\langle s_H | (\sigma_H / r_H^3)_0 | p_{\bar{\pi}O'} \rangle$, and $\langle p_{\bar{\pi}O} | \sigma_H / r_H^3 | p_{\bar{\pi}O'} \rangle$ are 0.0673, 0.0118, and 0.0094 au, respectively, where $p_{\bar{\pi}O'}$ AO lies on the HOO' plane and σ is the coordinate axis pointing from O to O'.

(40) Although by the localized orbital method we can construct from these σ and π lone pairs two identical lone pairs which bisect these original lone pairs, the physical meaning is not altered by this method. See, *e.g.*, C. Edmiston and K. Ruedenberg, *Rev. Mod. Phys.*, **35**, 457 (1963).

Table III. Stable Conformations and Barriers to Internal Rotation about the Single Bond[a]

Molecule	Stable conformation	Rotational barrier,[b] kcal/mol
HO—OH	111.5° from cis	V(cis) = 7.03, V(trans) = 1.10
HS—SH	90.6° from cis[c]	V(cis) = (7.4),[d] V(trans) = (1.9)[d]
H_2N—OH	Trans-staggered	V(from cis) = (2.53,[e] 1.16[f]), V(from trans) = (9.90,[e] 11.95[f])
H_2N—NH_2	90 ~ 95° from cis-eclipsed	V(cis) = (11.05,[e] 11.88,[f] 11.5[g]), V(trans) = (6.21,[e] 3.70,[f] 4.7[g])
H_3C—OH, H_3C—SH, H_3C—SeH	Staggered	V(CO) = 1.07, V(CS) = 1.27, V(CSe) = 1.01
H_3C—NH_2, H_3C—PH_2, H_3C—AsH_2	Staggered	V(CN) = 1.98, V(CP) = 1.96, V(CAs) = 1.32
H_3C—CH_3, H_3C—SiH_3, H_3C—GeH_3, H_3C—SnH_3	Staggered	V(CC) = 2.875, V(CSi) = 1.70, V(CGe) = 1.24, V(CSn) = ~0.65
H_3B—NH_3	Staggered	V = (3.29)[h]
HO—NO	Trans-planar	V(from cis) = 8.7, V(from trans) = 11.57
HO—CHO	Trans-planar	V = 13.4
H_3C—CHO	H eclipsing O[i]	V = 1.16
CH_2=HC—CH=CH_2	Trans-planar	V(from cis) = 2.6

[a] All the experimental values are cited from ref 22b, except where specially noted. [b] Values in parentheses are the theoretical values. [c] Reference 38. [d] Reference 33j. [e] Reference 33g. [f] Reference 33i. [g] Reference 33e. [h] M. Moireau and A. Veillard, *Theor. Chim. Acta*, **11**, 344 (1968). [i] Reference 37.

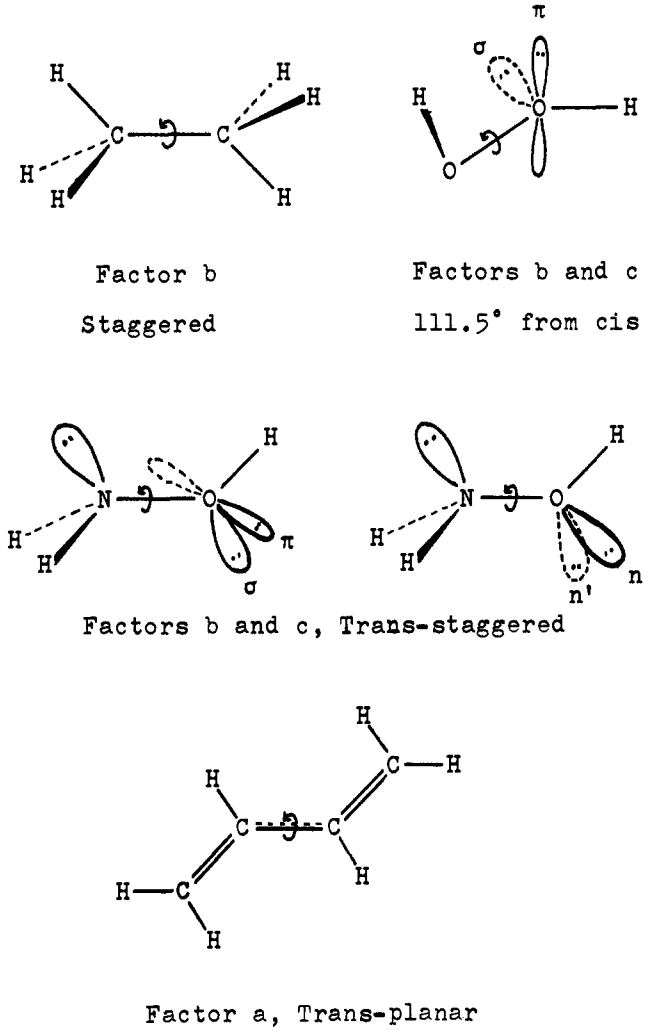

Figure 8. Examples of the important factors in the internal rotation about the single bond.

for the final conclusion. Thus, the present theory predicts the rotational angle θ to be 90–180° from cis (experiment, θ = 111.5°). From the above discussions, the fact is easily understood that the trans barrier is considerably smaller than the cis barrier (Table III). Similar considerations may also hold for H_2S_2. From *ab initio* SCF-MO calculations,[33f-h] it is generally known that the trans barrier of H_2O_2 is very difficult of reproduce. The reason seems to be due to the above delicateness. Another interesting example determined from both factors b and c is hydroxylamine, NH_2OH. Although both descriptions of lone-pair orbitals on oxygen shown in Figure 8 are equivalent from the localized orbital concept,[40] the right-hand-side is more convenient in this case. As may be clear from the figure, *both* factors b and c favor trans-staggered conformation. Then, the rotational barrier from this conformation is large (Table III). Similar considerations may hold for the molecules shown above BH_3NH_3 in Table III, except for NH_2NH_2 and perhaps for CH_3OH series. For these molecules, the factor a should also be taken into account (see Table II). However, for the molecules below HONO, the factor a is expected to be more important than the factors b and c, since the A–B bond has partial double bond character (the representative is butadiene shown in Figure 8). Their planar structures will be due to the orbital following discussed in the previous section.

Shapes of X_mABY_n Molecules

The shapes of X_mABY_n molecules[41,42] include two new problems in comparison with the previous AX_n molecules.[1] One is the effect of the BY_n fragment on the shape of the AX_m fragment and the other is the rotational problem about the A–B bond. The former problem is solved by considering the overlap effect, and the general features of the latter problem have been discussed in the previous sections. The shapes of the AX_m and BY_n fragments can be treated similarly to the previous papers.[1]

(i) HAAH Molecules and Their Derivatives. The shapes of HAAH molecules and their derivatives can be treated very similarly to the shapes of HAX molecules

(41) G. Herzberg, "Molecular Spectra and Molecular Structure, III. Electronic Spectra and Electronic Structure of Polyatomic Molecules," Van Nostrand, Princeton, N. J., 1965.
(42) L. E. Sutton, Ed., *Chem. Soc. Spec. Publ.*, No. 11 (1958); No. 18 (1965).

Table IV. Shapes of HAAH Molecules and Their Derivatives

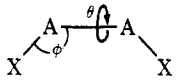

Shape[a]	Configuration $\bar{\pi}$	π	$\bar{\pi}^*$	π^*	Molecule (ϕ, θ)[b]
Linear	2	1	0	0	$HCCH^+$ [c,d]
Linear	2	2	0	0	HCCH,[c,e] HCCCl,[e] HCCBr,[e] ClCCCl,[e] BrCCBr[e]
Planar cis or trans	1	2	1	0	*HCCH (120°, trans)[c]
Planar cis or trans	2	2	2	0	HNNH (109°, trans)[f] FNNF (114.5°, cis)[g]
Nonplanar	2	2	2	2	HOOH (94.8, 119.8°)[h] HSSH (91.3, 90.6°)[i] FOOF (109.5, 87.5°)[j,k] FSSF (108.3, 87.9°)[l,k] ClSSCl (107, 82.5°)[e] BrSSBr (105, 83.5°)[e]

[a] $\theta = 0°$ at cis and $\theta = 180°$ at trans. [b] Values in parentheses are the angles ϕ and θ (ϕ, θ). The asterisk means that the molecule is in the excited state. [c] Reference 41. [d] Reference 43. [e] Reference 42. [f] A. Trombetti, *Can. J. Phys.*, **46**, 1005 (1968). [g] R. L. Kuczkowski and E. B. Wilson, Jr., *J. Chem. Phys.*, **39**, 1030 (1963); R. K. Bohn and S. H. Bauer, *Inorg. Chem.*, **6**, 309 (1967). [h] R. L. Redington, W. B. Olson, and P. C. Cross, *J. Chem. Phys.*, **36**, 1311 (1962). [i] Reference 38. [j] R. H. Jackson, *J. Chem. Soc.*, 4585 (1962). [k] W. H. Green and A. B. Harvey, *J. Chem. Phys.*, **49**, 3586 (1968). [l] R. L. Kuczkowski, *J. Amer. Chem. Soc.*, **86**, 3617 (1964).

discussed previously.[1] Table IV summarizes the experimentally known shapes. The MO density distributions of these molecules differ from Figure 2 of paper II only in that the n_σ MO is lowered than π and $\bar{\pi}$ MO's due to its stabilization by the formation of the A–H bond. Thus, for the electronic configurations $(\bar{\pi})^{0-2}(\pi)^{0-2}(\bar{\pi}^*)^0(\pi^*)^0$ (*e.g.*, $C_2H_2^+$,[43] C_2H_2), $D(p_{\pi A})$ and $D(p_{\bar{\pi}A})$ are less than or nearly equal to $1/(1+S) \simeq 0.8$ (overlap effect). Then, the shapes are expected to be linear. When π and $\bar{\pi}$ MO's are singly or doubly filled, the EC force increases due to the multiple bond character, which also favors linear structure. In the $\bar{\pi}$–$\bar{\pi}^*$ excited states of acetylene, $D(p_{\bar{\pi}A})$ becomes nearly equal to unity (see Table I). Then, the CCH fragments will become bent on the $\bar{\pi}$ plane, which results in a planar cis or trans structure.[41] Although the situation is very similar to that in CH_2 ($^3B_1$, 136°),[1] the CCH angle should be larger than the HCH angle due to the remaining π-overlap effect. For the configurations $(\bar{\pi})^2(\pi)^2(\bar{\pi}^*)^{1-2}(\pi^*)^0$, $D(p_{A\bar{\pi}}) > 1$. Then, the molecule should bend on the $\bar{\pi}$ plane, resulting in a planar cis or trans structure. If both $\bar{\pi}^*$ and π^* MO's are doubly filled (*e.g.*, H_2O_2, H_2S_2), both $D(p_{\bar{\pi}A})$ and $D(p_{\pi A})$ become larger than or nearly equal to two. Then, the molecule should be bent, but there is no large preference between $\bar{\pi}$ and π planes. The relative orientation of the two fragments is a sensitive problem and has been discussed in the previous section. Although the orbital following and preceding were not used here for the rotational problem, the planar structure of the molecules belonging to the configurations $(\bar{\pi})^1(\pi)^2(\bar{\pi}^*)^1(\pi^*)^0$ and $(\bar{\pi})^2(\pi)^2(\bar{\pi}^*)^{1-2}(\pi^*)^0$ can also be deduced from the orbital following.

(ii) HABX Molecules. The shapes of HABX molecules can be treated very similarly to the shapes of XAY molecules[44] discussed in paper II. The magnitudes of $D(p_{\bar{\pi}A})$ and $D(p_{\bar{\pi}B})$ are useful guides for the linear-bent problems of HAB and ABX fragments on the $\bar{\pi}$ plane. The MO density distributions of the HABX molecule differ from Figure 4 of paper II only in that the σ_u MO is lower than the π ($\bar{\pi}$) MO. (The atoms X and A in Figure 4 of paper II correspond to the atoms A and B of the present HABX molecules.) Table V gives the experimentally known shapes. If the molecule belongs to the configurations $(\bar{\pi}_g)^{0-1}(\pi_g)^{0-1}(\bar{\pi}_u^*)^0(\pi_u^*)^0$, both $D(p_{\pi A})$ ($D(p_{\bar{\pi}A})$) and $D(p_{\pi B})$ ($D(p_{\bar{\pi}B})$) are considerably less than unity. Then the molecule should be linear. No example is known experimentally for this class. For the electronic configurations $(\pi_u)^4(\bar{\pi}_g)^2(\pi_g)^{0-2}(\bar{\pi}_u^*)^0(\pi_u^*)^0$, $D(p_{\bar{\pi}A})$ and $D(p_{\bar{\pi}B})$ are calculated from Hückel MO's, including overlap for allyl,[9] to be 1.4 and 0.7 ($S = 0.25$), respectively. Then, the corresponding molecules are expected to take a planar structure in which the HAB fragment is bent and the ABX fragment is linear. This prediction agrees for the 15 and 16 valence electron molecules shown in Table V, except for HCCBr and HCCCl. The disagreement is due to the use of homopolar π MO's of allyl in calculating $D(p_{\bar{\pi}A})$. Ethylene π MO's will be a better first approximation for these molecules as treated in the previous section. For the electronic configurations $(\pi_u)^4(\bar{\pi}_g)^{1-2}(\pi_g)^{0-2}$ $(\bar{\pi}_u^*)^{1-2}(\pi_u^*)^0$, both $D(p_{\bar{\pi}A})$ and $D(p_{\bar{\pi}B})$ are larger than unity. Then, the shapes of both HAB and ABX fragments should become bent. Moreover, since the π_u^* MO is empty, the orbital following will occur when the molecule is rotated from the planar structure. Thus, the geometry should be a planar cis or trans structure. (See the 18 electron molecules shown in Table V.) If the number of valence electrons increases to take the configuration $(\pi_u)^4(\pi_g)^4(\pi_u^*)^4$ (20 valence electrons), the molecule will become nonplanar. A hypothetical example is HOOF. The rotational angle about the A–B bond will be discussed similarly to the previous section.

(iii) H_2ABH Molecules. Although the shape of H_2ABH molecules known experimentally are very few, they are summarized in Table VI. In the following designation, $p_{\pi A}$ and $p_{\pi B}$ AO's form π and π^* MO's between the A–B bond, and $p_{\bar{\pi}B}$ AO remains as the lone-

(43) W. A. Lathan, W. J. Hehre, and J. A. Pople, *J. Amer. Chem. Soc.*, **93**, 808 (1971).
(44) S. D. Peyerimhoff, *J. Chem. Phys.*, **47**, 349 (1967); see also, R. J. Buenker and S. D. Peyerimhoff, *Theor. Chim. Acta*, **24**, 132 (1972).

Table V. Shapes of HABX Molecules

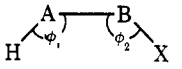

Shape[a]	No. of val elec	Configuration[b] $\bar{\pi}_g$	π_g	$\bar{\pi}_u^*$	π_u^*	Molecule (ϕ_1, ϕ_2)[c]
Planar	15	2	1	0	0	HNCN (116.5, 180°)[d]
Planar	15	1	2	0	0	*HNCN (120.6, 180°)[d]
Linear	16	2	2	0	0	HCCCl,[e] HCCBr[e]
Planar	16	2	2	0	0	HNCO (125.5, 180°)[e]
						HNCS (130.4, 180°)[e]
						HNNN (112.7, 180°)[f]
Planar cis or trans	18	2	2	2	0	HONO (104, 116°; trans)[e,g]
						HNSO (117.2°, ---)[h]

[a] See above representation. [b] All the molecules shown in the table have the configuration $(\bar{\pi}_u)^2(\pi_u)^2$. [c] Values in parentheses are the angles ϕ_1 and ϕ_2 (ϕ_1, ϕ_2). The asterisk means that the molecule is in the excited state. [d] Reference 41. [e] Reference 42. [f] E. H. Eyster, *J. Chem. Phys.*, **8**, 135 (1940); E. Ambre and B. P. Dailey, *ibid*, **18**, 1422 (1950). [g] Mean value of the values for cis and trans structures. [h] W. H. Kirchhoff, Ph.D. Thesis, Department of Chemistry, Harvard University, 1962 (quoted by R. L. Kuczkowski and E. B. Wilson, Jr., *J. Chem. Phys.*, **39**, 1030 (1963)).

Table VI. Shapes of H_2ABH Molecules

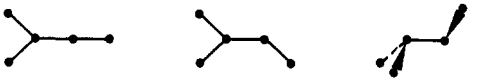

planar C_{2v} planar C_s nonplanar

Shape[a]	No. of val elec	Configuration π	$n_{\bar{\pi}B}$	π^*	H_2ABH
Planar C_{2v}	10	2	0	0	H_2CCH^+[b]
Planar C_s	11	2	1	0	H_2CCH[c]
Planar C_s	12	2	2	0	H_2CNH,[d] H_2COH^+[e]
Nonplanar	13	2	2	1	H_2COH[f]
Nonplanar	14	2	2	2	H_2NOH[g]

[a] See representations above. [b] Reference 45. [c] R. W. Fessenden and R. H. Schuler, *J. Chem. Phys.*, **39**, 2147 (1963); E. L. Cochran, F. J. Adrian, and V. A. Bowers, *ibid.*, **40**, 213 (1964). [d] D. E. Milligan, *ibid.*, **35**, 1491 (1961); C. B. Moore, G. C. Pimentel, and T. D. Goldfarb, *ibid.*, **43**, 63 (1965); see also J. M. Lehn and B. Munsch, *Theor. Chim. Acta*, **12**, 91 (1968). [e] G. A. Olah, D. H. O'Brien, and M. Calin, *J. Amer. Chem. Soc.*, **89**, 3582 (1967); see also P. Ros, *J. Chem. Phys.*, **49**, 4902 (1968). [f] W. T. Dixon and R. O. C. Norman, *J. Chem. Soc.*, 3119 (1963); A. J. Dobbs, B. C. Gilbert, and R. O. C. Norman, *Chem. Commun.*, 1353 (1969). [g] Trans-staggered conformation; ref 42 (see also ref 33g,i).

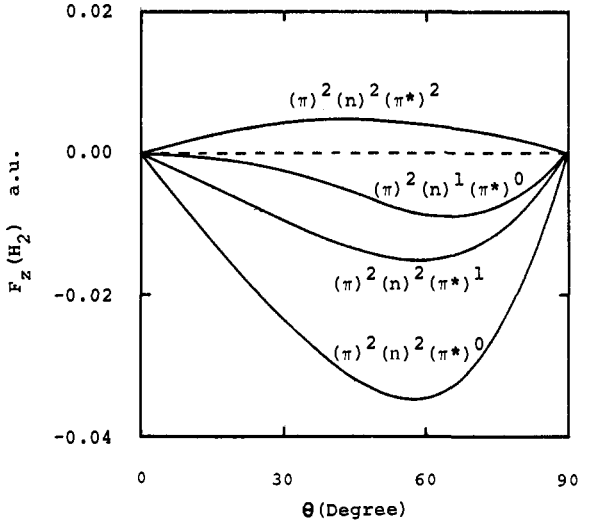

Figure 9. Curves of the rotational force, $F_z(H_2)$, *vs.* the twisting angle, θ, for the various electronic configurations arising from the extended Hückel MO's of vinyl, where the H_3 atom is missing in Figure 1.

pair orbital ($n_{\bar{\pi}B}$ MO). Their occupation numbers are also shown in Table VI. When the ABH fragment becomes bent, the problem of rotation about the A–B bond arises. Figure 9 gives the curves of the rotational

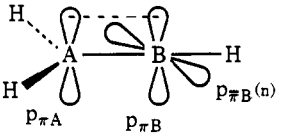

force *vs.* the twisting angle θ calculated for various electronic configurations arising from the extended Hückel MO's of vinyl.[29] The notations and geometry are the same as those in Figure 1, except that the H_3 atom is missing for vinyl. In Figure 9, positive and negative signs correspond to the promoting and restoring forces for the twisting motion from the planar structure. If the slope of the curve at $F_z(H_2) = 0$ is negative (positive), the angle corresponds to the stable minimum (unstable maximum) point in the potential curve. Table VII shows the analysis of the rotational force at $\theta = 45°$ due to eq 3 and 4.

For vinyl cation, $D(p_{\pi A})$, $D(p_{\pi B}) < 1$ and $D(p_{\bar{\pi}B}) \simeq 0$. Then, the shape should be planar C_{2v}, as experimentally pointed out indirectly.[45] For vinyl radical, $D(p_{\pi A})$, $D(p_{\pi B}) < 1$ and $D(p_{\bar{\pi}B}) \simeq 1$. Then, the H_2CC fragment should be planar and the CCH fragment should be bent. When these fragments are twisted from the planar structure, relatively small orbital

(45) D. R. Kelsey and R. G. Bergman, *J. Amer. Chem. Soc.*, **92**, 228 (1970); see also R. Hoffmann, *J. Chem. Phys.*, **40**, 2480 (1964); T. Yonezawa, H. Nakatsuji, and H. Kato, *J. Amer. Chem. Soc.*, **90**, 1239 (1968); ref 43.

Table VII. Analyses of the Rotational Force, $F_z(H_2)$ (au), at $\theta = 45°$ for Various Electronic Configurations Arising from Vinyl MO's

Force[a]	Electronic configuration $(\pi)^2(n)^1(\pi^*)^0$	$(\pi)^2(n)^2(\pi^*)^0$	$(\pi)^2(n)^2(\pi^*)^1$	$(\pi)^2(n)^2(\pi^*)^2$
Total	−0.0057	−0.0322	−0.0136	0.0049
	(i) First Analysis (Eq 3)			
Electronic part	−0.0097	−0.0363	−0.0177	0.0008
Nuclear part	0.0041	0.0041	0.0041	0.0041
	(ii) Second Analysis (Eq 4)			
EC(C_1–H_2) force	−0.0109	−0.0276	−0.0105	0.0067
EC(other) force	0.0012	0.0015	0.0003	−0.0010
EGC force	0.0040	−0.0061	−0.0034	−0.0007

[a] The analyses are due to eq 3 and 4. The notations of the forces are the same as those in Table II.

following will occur.[46] This is confirmed in Table VII from the EC force on H_2 due to the C_1–H_2 bond-electron distribution. The total rotational force is plotted in Figure 9. From these, the molecule is expected to take the planar C_s structure. For H_2CNH and H_2COH^+, the structure will be planar C_s from similar reasons as for the vinyl radical. But, the extent of bending of the ABH fragment should increase since $D(p_{\bar{\pi}B}) \simeq 2$ in this case. The extent of the orbital following will also increase,[46] which is confirmed in Table VII. For H_2COH, all the magnitudes of $D(p_{\pi A})$, $D(p_{\pi B})$, and $D(p_{\bar{\pi}B})$ are considerably larger than unity. Then, the shape will become nonplanar. From Table VII and Figure 9, the orbital following will cause the relative orientation of the two fragments to be near 90° from the cis-staggered conformation, for which no experimental evidence is yet known. For H_2NOH, all the magnitudes of $D(p_{\pi A})$, $D(p_{\pi B})$, and $D(p_{\bar{\pi}B})$ are near two, and the shape should become nonplanar. The rotational problem about the single bond has been discussed in the previous section. Figure 9 also supports the staggered conformation.

(iv) H_2AAH_2 Molecules and Their Derivatives. Shapes of H_2AAH_2 molecules and their derivatives are summarized in Table VIII. First, the shapes of AH_2 fragments are discussed, and then the rotational problem about the A–A bond is discussed. From similar considerations on HAAH molecules, if the molecule belongs to the electronic configurations $(\pi)^{0-2}(\pi^*)^0$, $D(p_{\pi A}) < 1$, and the shape of the AH_2 fragment will be planar. The prediction agrees for all the molecules above CF_2CF_2 in Table VIII. The shape of $CH_2B(Me)_2$, isoelectronic with $CH_2CH_2^+$, was also reported from esr measurement to be planar at both carbon and boron.[47] For the π–π^* excited state $(\pi)^1(\pi^*)^1$, $D(p_{\pi A}) \simeq 1$. Then, the shape of the AH_2 fragment will be a result of the critical balance of the AD and EC forces as seen previously for CH_3.[1] Then, although the shape is expected to be planar or nearly planar, it will be affected sensitively by the central atom effect, substituent effect, etc. Actually, Burnelle and Litt[48] suggested from semiempirical calculations a possibility that the CH_2 fragment of the π–π^* excited state of ethylene might be pyramidal in the triplet state but planar in the singlet state. For the configurations $(\pi)^2(\pi^*)^{1-2}$, $D(p_{\pi A}) > 1$, and the shape of the AH_2 fragment will become pyramidal. The extent of bending will increase from $(\pi)^2(\pi^*)^1$ to $(\pi)^2(\pi^*)^2$. For this prediction, only one disagreement is seen for $NH_2NH_2^+$.

From esr measurements, Brivati, *et al.*,[49a] and Edlund, *et al.*,[49b] reported the shape of $NH_2NH_2^+$ to be nearly planar. This is a first example of the serious disagreement of the ESF theory with experiment throughout papers I–III. Since $D(p_{\pi N})$ of $NH_2NH_2^+$ is calculated from Table I to be $(3 - S)/2(1 - S^2) \simeq 1.5$, which is considerably larger than unity, the possible σ-overlap effect seems insufficient to account for the planarity. Thus, we actually calculated the potential curve of this molecule by other theoretical methods such as the extended Hückel method and the INDO–UHF method.[50] The former calculated the shape to be planar, but the latter calculated it to be nonplanar with

Table VIII. Shapes of H_2AAH_2 Molecules and Their Derivatives[a]

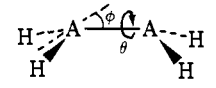

Shape	Configuration π	π^*	Molecule (ϕ, θ)[b]
Bisected	0	0	F_2BBF_2 (0, 90°),[c] Cl_2BBCl_2 (0, 90°)[d]
Staggered	1	0	$H_2CCH_2^+$ (0, ∼30°),[e,f] Rydberg excited H_2CCH_2 (0, 25°)[f]
Planar	2	0	H_2CCH_2 (0, 0°),[g] F_2CCF_2 (0, 0°)[g]
Bisected	1	1	π–π^* excited H_2CCH_2 (---, 90°)[h]
Planar	2	1	$H_2NNH_2^+$ (∼0, 0°)[i]
Nonplanar	2	1	H_2CNH_2[j]
Nonplanar	2	2	H_2NNH_2 (51.6, 90–95°),[g] F_2NNF_2 (66.7, 65°)[g]

[a] $\theta = 0°$ at cis eclipsed. The terms "bisected" and "staggered" are distinguished in this table; the former corresponds to the shape $\phi = 0°, \theta = 90°$ and the latter to the shape $\phi = 0°, \theta = 0°$. [b] Values in parentheses show the angles ϕ and θ (ϕ, θ). [c] Reference 27. [d] Reference 28. [e] References 55 and 57. [f] Reference 56. [g] Reference 42. [h] Reference 25 (see also ref 48). [i] Reference 49, (see also the discussions given in the text). [j] References 47 and 53 (see also the discussions given in the text).

(46) The EC force due to the orbital following should be relatively small in the vinyl radical, since the numbers of electrons assigned to $p_{\pi B}$ and n orbitals are both unity. The orbital following is due to the difference in the overlap interactions between $p_{\pi A}$ and $p_{\pi B}$ AO's at $\theta = 0°$ and between $p_{\pi A}$ and n orbitals at $\theta = 90°$. The former is larger than the latter. However, when the occupation number of n orbital becomes two as in CH_2NH, the antibonding interaction occurs between $p_{\pi A}$ and n orbitals at $\theta = 90°$. Then, in this case, the extent of the orbital following should be larger than that in the vinyl radical. This is ascertained in Table VII.

(47) A. R. Lyons and M. C. R. Symons, *J. Chem. Soc. Faraday Trans.*, 2, 502 (1972).

(48) L. Burnelle and C. Litt, *Mol. Phys.*, 9, 433 (1965); see also ref 4, p 2325.

(49) (a) J. A. Brivati, J. M. Gross, M. C. R. Symons, and D. J. A. Tinling, *J. Chem. Soc.*, 6504 (1965); (b) O. Edlund, A. Lund, and A. Nilsson, *J. Chem. Phys.*, 49, 749 (1968).

(50) J. A. Pople and D. L. Beveridge, "Approximate Molecular Orbital Theory," McGraw-Hill, N. Y., 1970.

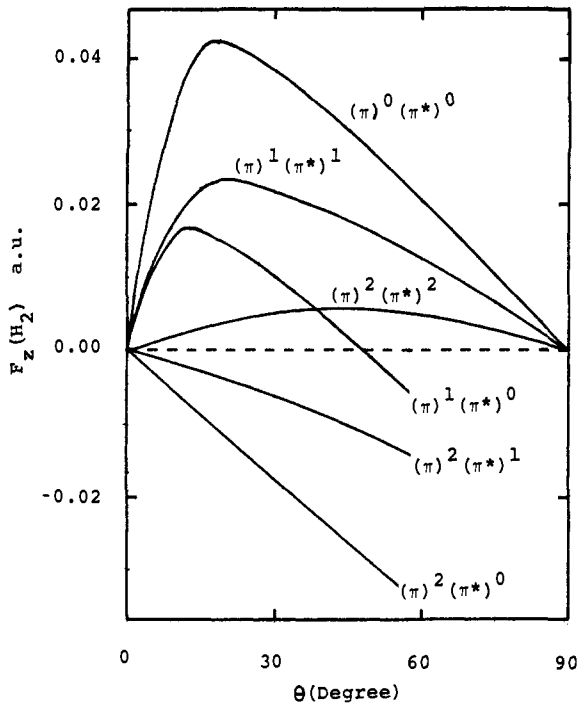

Figure 10. Curves of the rotational force, $F_z(H_2)$, *vs.* the twisting angle, θ, for the various electronic configurations arising from ethylenic MO's calculated by the extended Hückel method. Since π and π^* MO's become degenerate at $\theta = 90°$, the plot is given only in the region $0° \leq \theta \leq 45°$ for the configurations $(\pi)^1(\pi^*)^0$, $(\pi)^2(\pi^*)^0$, and $(\pi)^2(\pi^*)^1$.

the out-of-plane angle $\phi = \sim 30°$.[51] Between these two methods, the INDO–UHF method is generally more reliable for this problem,[50] especially since $NH_2NH_2^+$ is an open-shell molecule.[52] On the other hand, for the isoelectronic radical CH_2NH_2, nonplanarity has been suggested from the esr measurements.[47,53] From comparison of the observed hfs constants with those calculated from INDO MO's, Wood and Lloyd[53a] reported the geometry to be the nonplanar trans conformation with the out-of-plane angle of $\sim 25°$ at carbon and $\sim 40°$ at nitrogen. Neta and Fessenden[53b] also suggested nonplanarity at the carbon. However, Lyons and Symons[47] objected to these and suggested that the radical is locally planar at carbon but slightly pyramidal at nitrogen. The present theory prefers the result of Wood and Lloyd as discussed above. However, considering these situations, we think that more detailed examinations are necessary for the shapes of $NH_2NH_2^+$, CH_2NH_2, and other $(\pi)^2(\pi^*)^1$ molecules from both theoretical and experimental standpoints before final conclusions are made.

For the rotational problem about the A–A bond, general features were already discussed in the previous section. In Figure 10, the dependence of the rotational force, $F_z(H_2)$, on the twisting angle θ is shown for the various electronic configurations arising from ethylenic MO's calculated from the extended Hückel method[29] (see also Figure 1). Since π and π^* MO's become degenerate at $\theta = 90°$, the plot is given only in the region $0° \leq \theta \leq 45°$ for the configurations $(\pi)^1(\pi^*)^0$, $(\pi)^2(\pi^*)^0$, and $(\pi)^2(\pi^*)^1$. The orbital following and preceding were ascertained respectively for the negative and positive regions of Figure 10 from the same examinations as Table II.

For the electronic configurations $(\pi)^0(\pi^*)^0$ and $(\pi)^1(\pi^*)^1$, the rotational angle θ is expected to be 90° (bisected). For the configurations $(\pi)^2(\pi^*)^0$ and $(\pi)^2(\pi^*)^1$, the rotational angle will be 0° (planar or nonplanar cis or trans). These results agree with the experimental findings shown in Table VIII.[54] Interestingly, for the configuration $(\pi)^1(\pi^*)^0$, the stable rotational angle is found near 45°. This agrees with the theoretical predictions[55] and with the experimental findings due to Merer and Schoonveld.[56,57] They reported from spectral analysis that the rotational angle of the first Rydberg excited state of ethylene is near 25° and suggested similar possibility for the ethylene cation. The analysis of force due to eq 4 revealed that when $0° < \theta < 40°$, the orbital preceding occurs, but when $\theta > 40°$, the orbital following occurs. This is the reason for the calculated stable rotational angle to be near 45°. For the configuration $(\pi)^2(\pi^*)^2$, Figure 10 gives the result that the rotational angle will be 90° (bisected), which agrees with the experimental shape of NH_2NH_2 and NF_2NF_2.

Concluding Remarks

In the present paper, an extension is made on the ESF theory proposed in paper I. First, the overlap effect on the AD and EC forces is examined. The effect is proved to have wide applicabilities for both molecular structure and chemical reaction. Especially, the overlap effect on the EC force is shown to manifest itself in many important aspects of chemical reaction and molecular interaction (see Table I). Another manifestation of the overlap effect is the orbital following and preceding found from the consideration on the internal rotation problems. Actually, they are proved to be the dominant origin of the rotational barrier in many important cases, except for the rotation about the single bond, for which general features are also discussed. Three factors are pointed out to be important. Based on the considerations summarized above and in the previous papers,[1] we discussed the shapes of X_mABY_n molecules. The results were generally satisfactory.

As seen in the rotational problem of ethylene, energetic consideration does not always necessitate the concept of orbital following and preceding. This seems the actual reason of the overlook of these important features of electron-density distribution except for some investigations.[30–32] Since in the ESF theory the knowledge on the manner of electron distribution has a unique importance in comparison with other (en-

(51) The INDO-UHF calculation of ethylene anion isoelectronic with $NH_2NH_2^+$ also predicted the shape to be nonplanar.

(52) H. W. Kroto and D. P. Santry, *J. Chem. Phys.*, **47**, 792, 2736 (1967); see also R. J. Buenker and S. D. Peyerimhoff, *ibid.*, **53**, 1368 (1970).

(53) (a) D. E. Wood and R. V. Lloyd, *ibid.*, **53**, 3932 (1970); (b) P. Neta and R. W. Fessenden, *J. Phys. Chem.*, **75**, 738 (1971).

(54) The rotational angle θ of ethylene anion was calculated to be 90° by the nonempirical LCAO-SCF calculations due to Kaldor and Shavitt (ref 55b). However, they did not examine the shape of the CH_2 fragment (see also ref 51).

(55) (a) R. S. Mulliken, *Tetrahedron*, **5**, 253 (1959); (b) U. Kaldor and I. Shavitt, *J. Chem. Phys.*, **48**, 191 (1968).

(56) A. J. Merer and L. Schoonveld, *ibid.*, **48**, 522 (1968); *Can. J. Phys.*, **47**, 1731 (1969).

(57) A. J. Merer and R. S. Mulliken, *Chem. Rev.*, **69**, 639 (1969).

ergetic) theories, these orbital following and preceding become so much the more important. These orbital following and preceding seem to have a general importance in that they should appear in every chemical phenomena including the changes in nuclear configurations. Actually, the generality can be proved directly from the Hellmann–Feynman theorem.[21b] Since the orbital following and preceding act respectively to restrain and to promote the movement of nuclear configurations, the former will occur in the movement from stable configurations[58] and the latter will occur as one of the driving forces of the movement. These points will be studied more fully in the succeeding articles.[21]

For the internal rotation about the single bond, the calculation on ethane due to Goodisman[35a] showed that the Hellmann–Feynman force cannot always give good qualitative values, if an approximate wave function is used. However, we believe that the conceptual picture is another thing and can be obtained from the ESF theory, since the basic Hellmann–Feynman theorem is exact for exact wave functions. From this standpoint, the relative importance of the three factors is very interesting and will be examined more fully in another article.

(58) For the methyl radical, the orbital following which occurs when the radical is distorted from planar structure (ref 30b, 31, and 32), causes the EC force on the proton which acts to restore the radical to planar structure. The function is parallel with that of the EC force on the carbon discussed previously.[1]

Acknowledgment. The author wishes to acknowledge Professors T. Yonezawa and H. Kato and Dr. T. Kawamura for encouragement and valuable discussions, and Dr. H. Fujimoto and Mr. S. Yamabe for lending the author their program for the calculation of the density map. He also thanks the members of the Quantum Chemistry Group of his Department for useful discussions.

Molecular Properties of the Triatomic Difluorides BeF_2, BF_2, CF_2, NF_2, and OF_2

Stephen Rothenberg*[1a] and Henry F. Schaefer III*[1b]

Contribution from Information Systems Design, Oakland, California 94621, and the Department of Chemistry, University of California, Berkeley, California 94720. *Received October 20, 1972*

Abstract: Nonempirical self-consistent-field calculations have been carried out for the electronic ground states of BeF_2, BF_2, CF_2, NF_2, and OF_2. A contracted gaussian basis set of double ζ plus polarization quality was employed. For each molecule the following molecular properties were computed: dipole moment, quadrupole moment, octupole moment, second and third moments of the electronic charge distribution, diamagnetic susceptibility, diamagnetic shielding, and electric field gradient. In addition the electronic structures are discussed in terms of orbital energies and population analyses. For OF_2 comparison is made with experiment. The calculated and experimental values are $\mu = 0.45$ D (0.30), $\theta_{xx} = 0.61 \times 10^{-26}$ esu cm^2 (2.1 ± 1.1), $\theta_{yy} = -0.41$ (-1.6 ± 1.4), $Q_{xx} = 7.2 \times 10^{-16}$ cm^2 (6.9), $Q_{yy} = 25.1$ (25.2), $Q_{zz} = 3.1$ (3.0), $\chi_{xx}^{d} = -119.4 \times 10^{-6}$ erg/(G^2 mol) (-119.7), $\chi_{yy}^{d} = -43.5$ (-42.0), and $\chi_{zz}^{d} = -136.9$ (-136.2). The agreement is generally seen to be quite good, and it is hoped that the predicted but experimentally undetermined properties for the other molecules are equally reliable.

Perhaps the simplest and yet the most powerful intuitive device available to the chemist is the periodic table. A simple knowledge of trends expected to arise from moving up or down (or to the left or right) along the periodic table allows sensible predictions of the properties of a vast number of molecules which may be difficult to observe in the laboratory. Further, to better train his intuition, the chemist will frequently carry out experiments on a group of molecules in which a particular atom is substituted by neighboring atoms in the periodic table. Thus, ascertaining the exact nature of the differences between, for example, CH_3F, CH_3Cl, CH_3Br, and CH_3I, is a matter of enduring scientific interest.

The theoretical chemist would also like to study the electronic structure of periodically related groups of molecules. And, this can be done now if semiempirical methods are used.[2a] Furthermore, with the rapid development[2b] of new theoretical and computational methods, it seems likely that systematic *ab initio* studies of entire series of molecules will become commonplace during the next 10 years. It should be pointed out that Pople and coworkers[3] have already adopted a boldly systematic *ab initio* approach to the electronic structure of organic compounds. In the present paper we make a small step toward a systematic *ab initio* understanding of periodic properties. We report a self-consistent-field study of the first-row difluorides, BeF_2, BF_2, CF_2, NF_2, and OF_2. All five of these molecules have been observed in the laboratory[4–8]

(1) (a) Information Systems Design; supported by a grant from the ISD Internal Research Fund. (b) University of California; Alfred P. Sloan Fellow; supported by the National Science Foundation, Grant GP-31974.

(2) (a) M. Orchin and H. H. Jaffé, "Symmetry, Orbitals, and Spectra," Wiley-Interscience, New York, N. Y., 1971; (b) H. F. Schaefer, "The Electronic Structure of Atoms and Molecules: A Survey of Rigorous Quantum Mechanical Results," Addison-Wesley, Reading, Mass., 1972.

(3) L. Radom, W. A. Lathan, W. J. Hehre, and J. A. Pople, *J. Amer. Chem. Soc.*, **93**, 5339 (1971).

(4) BeF_2: A. Snelson, *J. Phys. Chem.*, **70**, 3208 (1966).

(5) BF_2: W. Nelson and W. Gordy, *J. Chem. Phys.*, **51**, 4710 (1969).

(6) CF_2: C. W. Mathews, *Can. J. Phys.*, **45**, 2355 (1967).

(7) NF_2: R. K. Bohn and S. H. Bauer, *Inorg. Chem.*, **6**, 304 (1967).

(8) OF_2: L. Pierce, N. Di Cianni, and R. H. Jackson, *J. Chem. Phys.*, **38**, 730 (1967).